

Table S1. MRI Sequences and Parameters

Parameters	T1WI	T2WI	DWI	CE-MRI
Sequence name	mDixion	FSE	EPI	VIBE
Orientation	Axial	Axial	Axial	Axial
Breath technique	Free breath	Free breath	Free breath	Free breath
TR/TE (ms)	5.48/2.46	700/97	1700/75	3.92/1.39
FOV (mm ²)	380 × 380	380 × 380	380 × 380	380 × 380
Matrix	156 × 156	174 × 132	152 × 150	256 × 192
Slice thickness/gap (mm)	4/1	4/1	6/1	2/1
Flip angle (degrees)	10°	90°	90°	10°
Bandwidth (Hz/pixel)	500	482	2442	400
NEX	1	1	1	1
b value (s/mm ²)	—	—	0, 800	—
Scanning time (s)	14	23	37	68

T1WI = T1-weighted imaging; T2WI = T2-weighted imaging; DWI = diffusion-weighted imaging, CE = contrast-enhanced; TSE = turbo spin echo; FSE = fast spin echo; EPI = echo planar imaging; VIBE = volumetric interpolated breath-hold examination; TR = repetition time; TE = echo time; FOV = field of view.

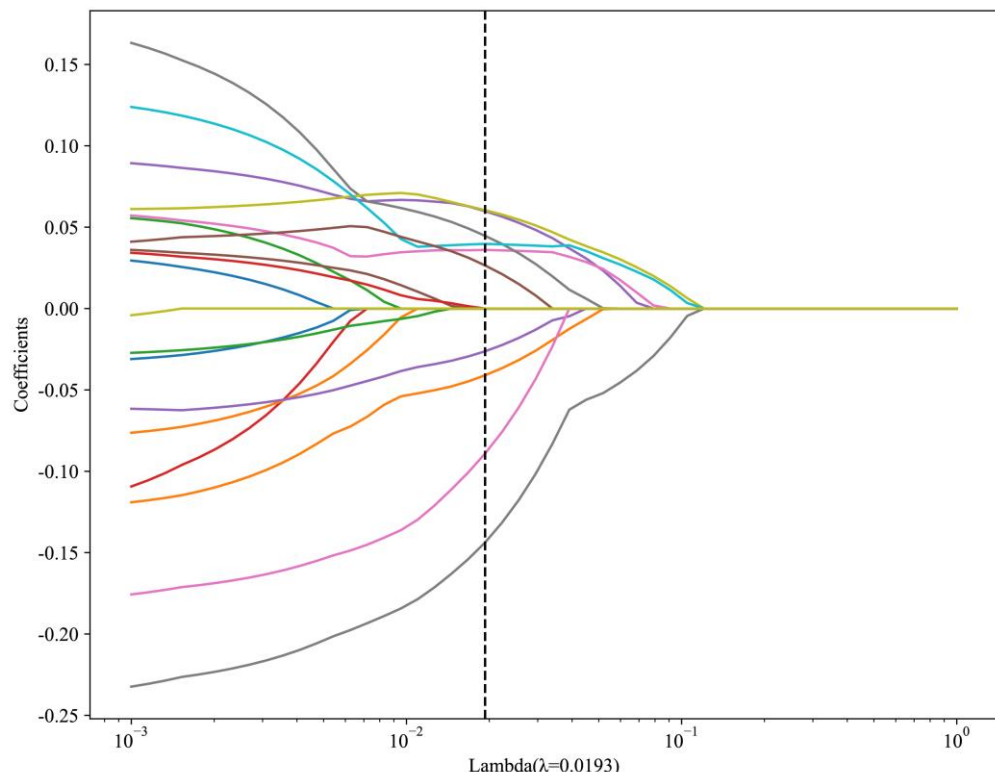


Figure. S1 LASSO result of radiomic model for predicting high Ki-67 expression in HCC

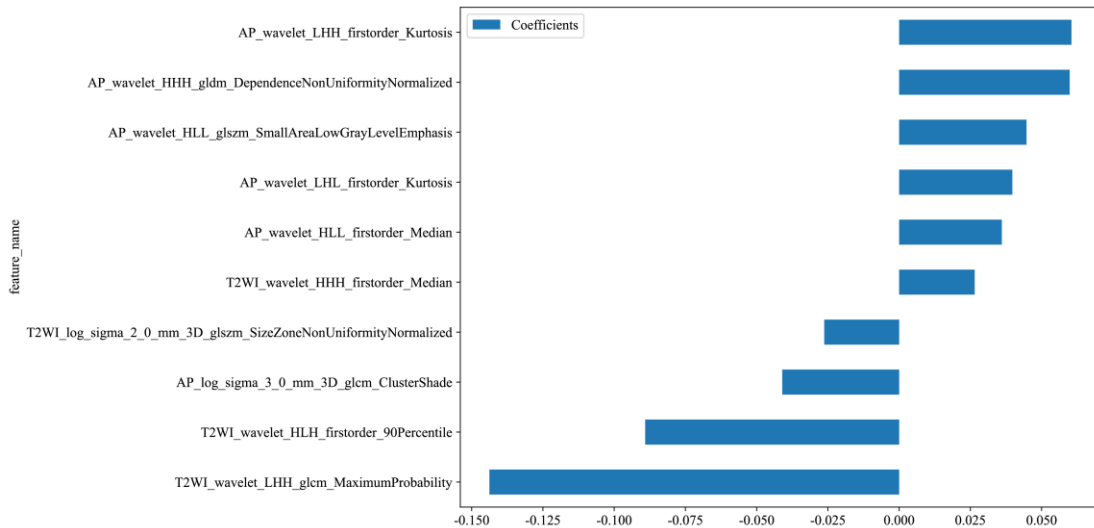


Figure. S2 Weighted importance of selected radiomic signatures

Table S2. The calculated formula of radiomic signatures

Rad-score = 0.4420289855072464

$$\begin{aligned}
 & -0.041007 * AP_log_sigma_3_0_mm_3D_glcm_ClusterShade \\
 & +0.059839 * AP_wavelet_HHH_gldm_DependenceNonUniformityNormalized \\
 & +0.036037 * AP_wavelet_HLL_firstorder_Median \\
 & +0.044709 * AP_wavelet_HLL_glszm_SmallAreaLowGrayLevelEmphasis \\
 & +0.060468 * AP_wavelet_LHH_firstorder_Kurtosis \\
 & +0.039731 * AP_wavelet_LHL_firstorder_Kurtosis \\
 & -0.026270 * T2WI_log_sigma_2_0_mm_3D_glszm_SizeZoneNonUniformityNormalized \\
 & +0.026518 * T2WI_wavelet_HHH_firstorder_Median \\
 & -0.089103 * T2WI_wavelet_HLH_firstorder_90Percentile \\
 & -0.143768 * T2WI_wavelet_LHH_glcm_MaximumProbability
 \end{aligned}$$

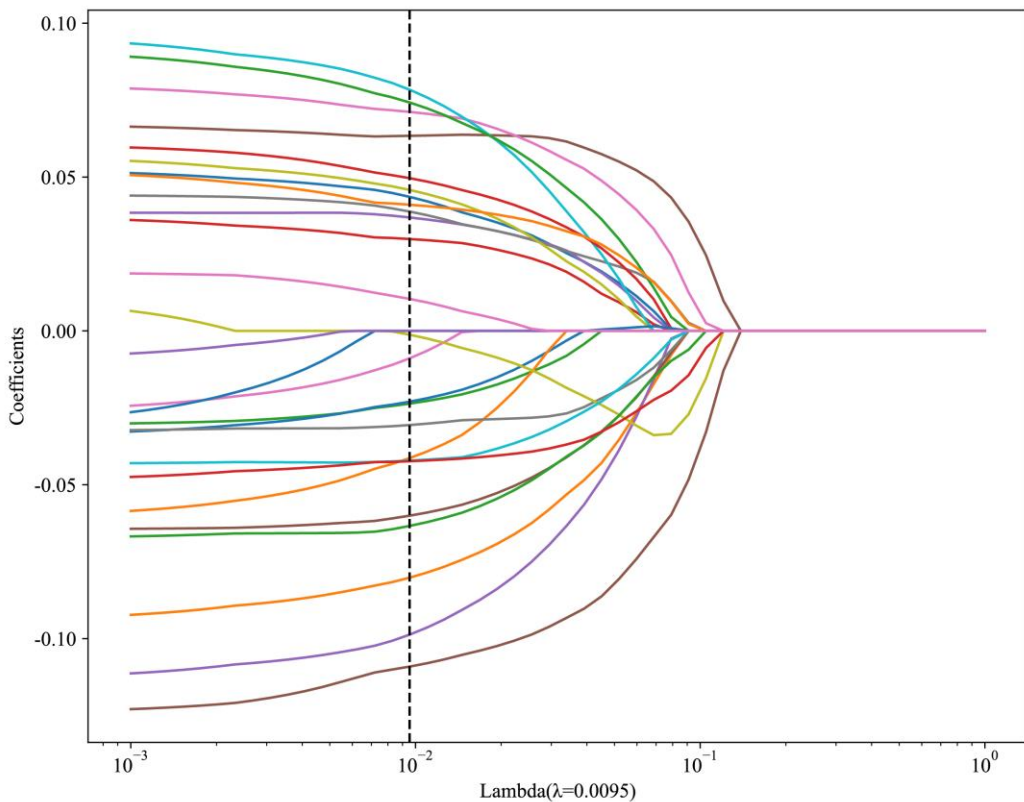


Figure. S3 LASSO result of DTL model for predicting high Ki-67 expression in HCC

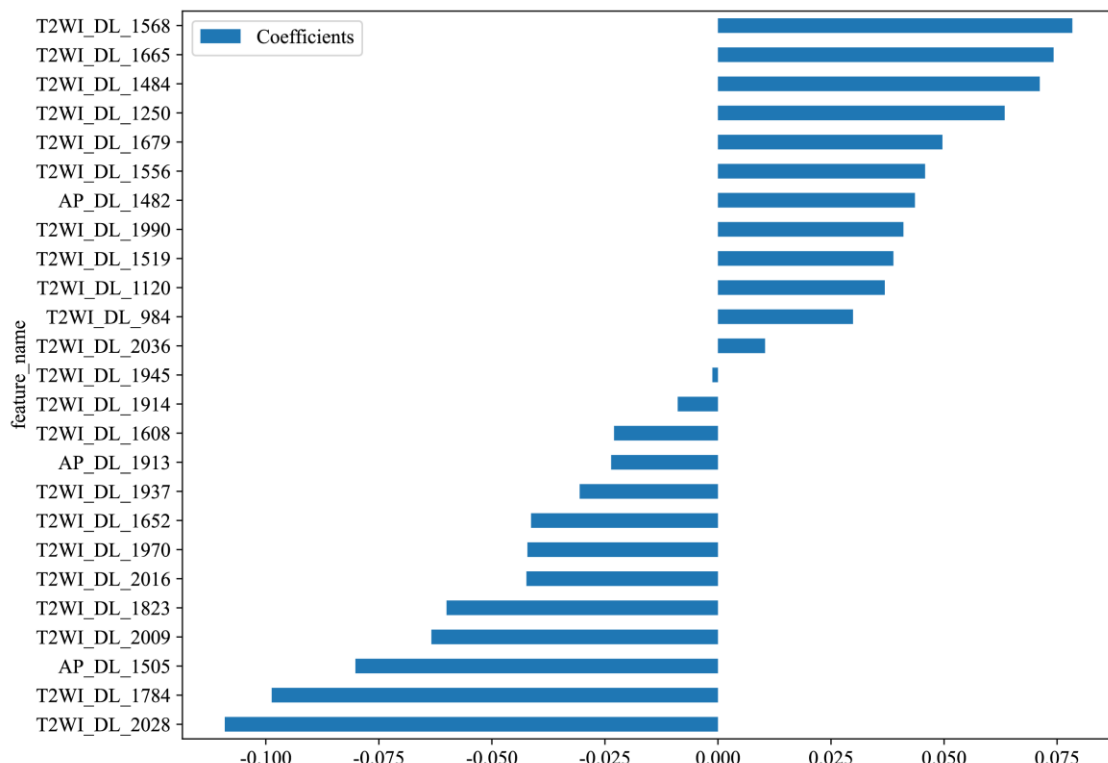


Figure. S4 Weighted importance of selected radiomic signatures

Table S3. The calculated formula of DTL signatures

Rad-score = 0.44202898550724634 +0.043560 * AP_DL_1482 -0.080176 * AP_DL_1505
 -0.023627 * AP_DL_1913 +0.029858 * T2WI_DL_984 +0.036873 * T2WI_DL_1120
 +0.063397 * T2WI_DL_1250 +0.071170 * T2WI_DL_1484 +0.038785 * T2WI_DL_1519
 +0.045807 * T2WI_DL_1556 +0.078369 * T2WI_DL_1568 -0.022987 * T2WI_DL_1608
 -0.041336 * T2WI_DL_1652 +0.074228 * T2WI_DL_1665 +0.049642 * T2WI_DL_1679
 -0.098693 * T2WI_DL_1784 -0.060040 * T2WI_DL_1823 -0.008903 * T2WI_DL_1914
 -0.030582 * T2WI_DL_1937 -0.001239 * T2WI_DL_1945 -0.042142 * T2WI_DL_1970
 +0.041006 * T2WI_DL_1990 -0.063374 * T2WI_DL_2009 -0.042350 * T2WI_DL_2016
 -0.109085 * T2WI_DL_2028 +0.010405 * T2WI_DL_2036

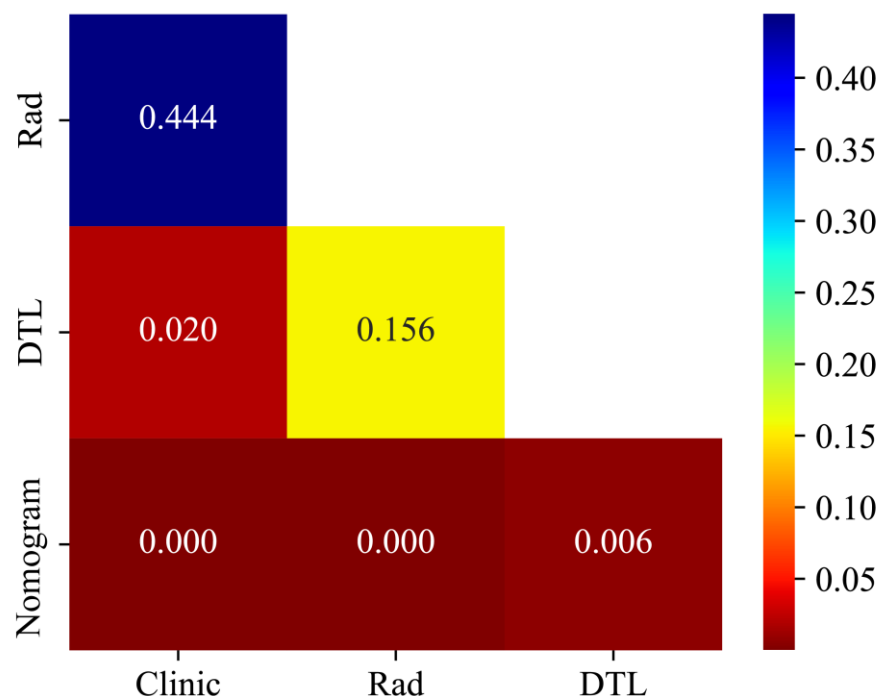


Figure. S5 Delong results of all predictive model in the training group

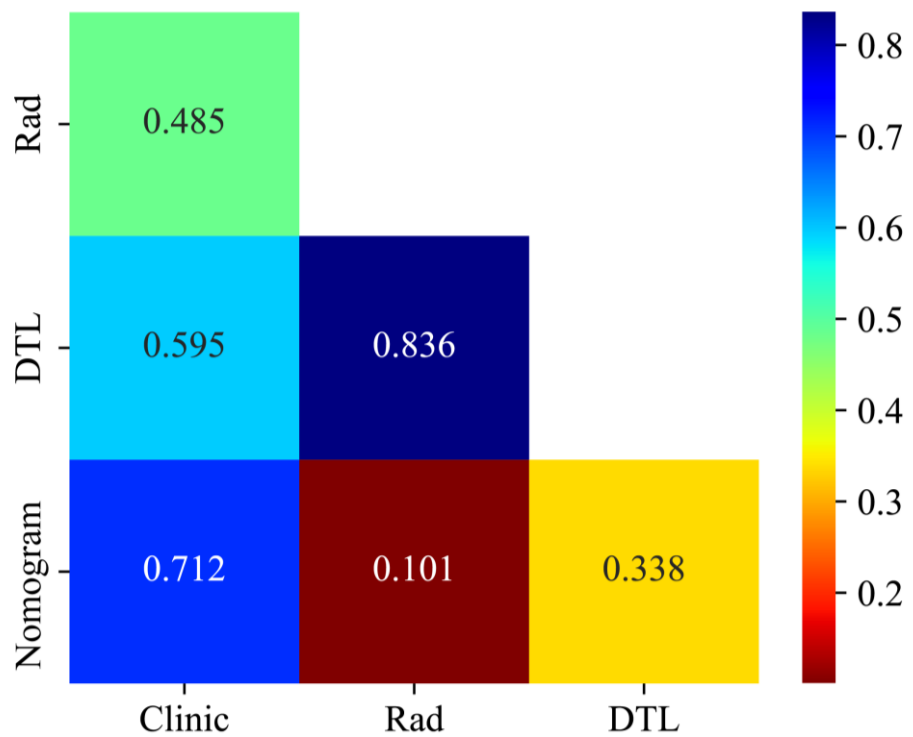


Figure. S6 Delong results of all predictive model in the validation group

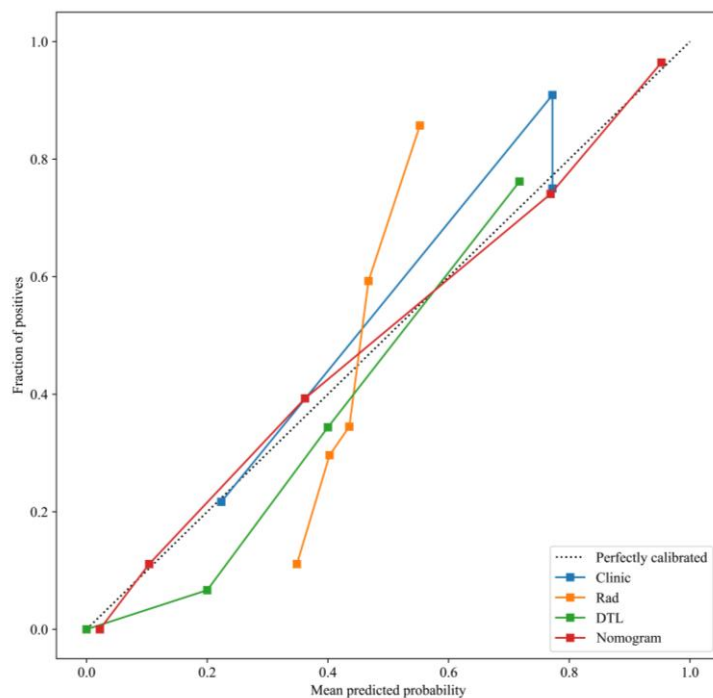


Figure. S7 Hosmer-Lemeshow (H-L) curves of all predictive model in the Training group

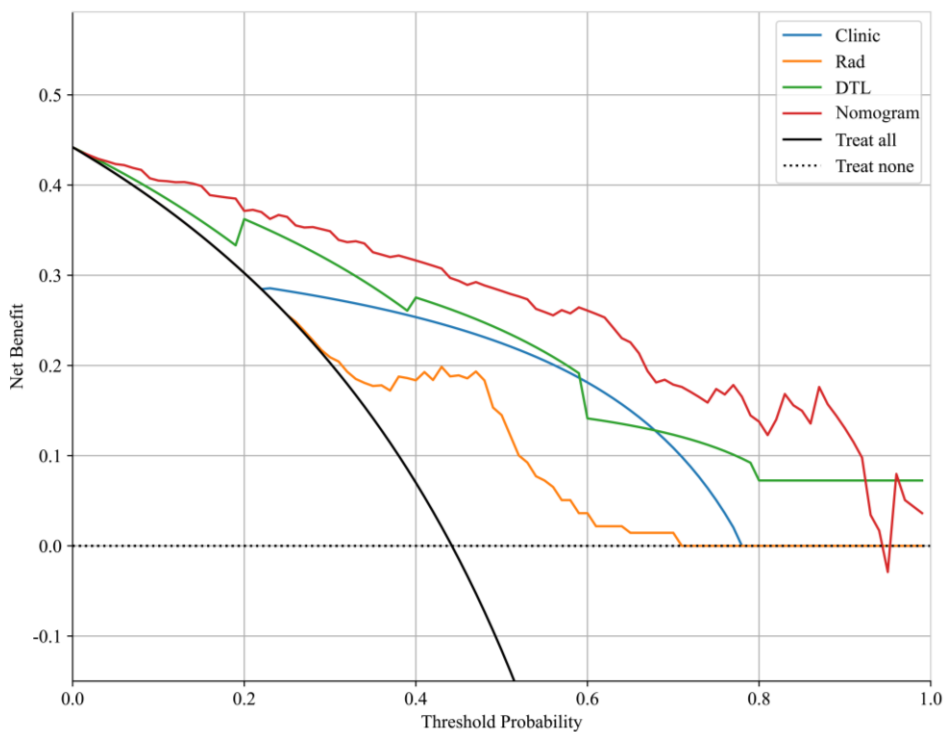


Figure. S8 Decision Curve Analysis (DCA) curves of all predictive model in the training group

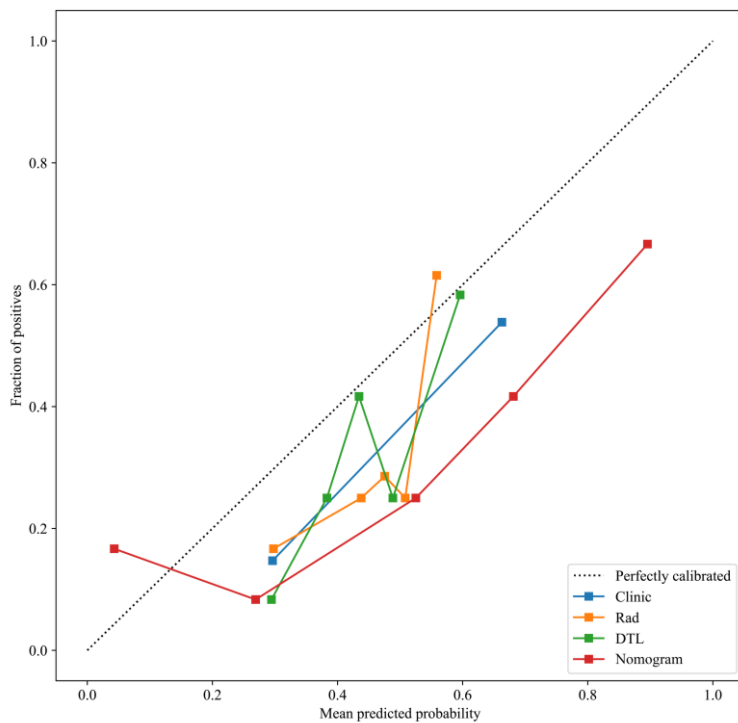


Figure. S9 Hosmer-Lemeshow (H-L) curves of all predictive model in the validation group

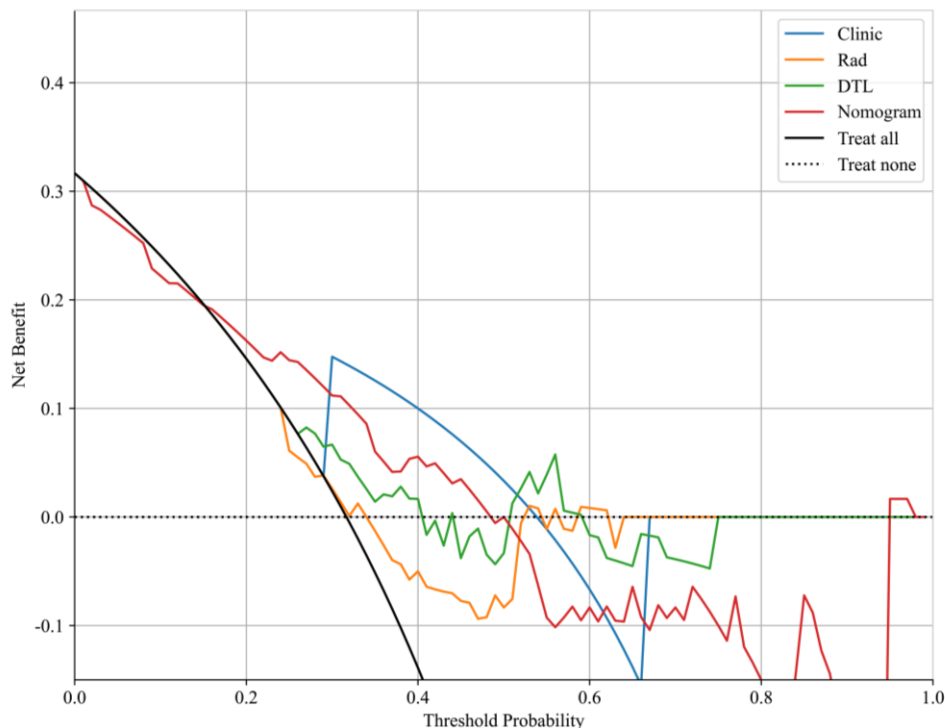


Figure. S10 Decision Curve Analysis (DCA) curves of all predictive model in the validation group